

Resonant interaction of trapped cold atoms with a magnetic cantilever tip

Cris Montoya, Jose Valencia, and Andrew A. Geraci*

*Department of Physics, University of Nevada, Reno, Nevada 89557, USA*Matthew Eardley, John Moreland, Leo Hollberg,[†] and John Kitching
National Institute of Standards and Technology, Boulder, Colorado 80305, USA

(Received 30 March 2015; published 26 June 2015)

Magnetic resonance in an ensemble of laser-cooled trapped Rb atoms is excited using a microcantilever with a magnetic tip. The cantilever is mounted on a multilayer chip designed to capture, cool, and magnetically transport cold atoms. The coupling is observed by measuring the loss from a magnetic trap as the oscillating cantilever induces Zeeman-state transitions in the atoms. Interfacing cold atoms with mechanical devices could enable probing and manipulating atomic spins with nanometer spatial resolution and single-spin sensitivity, leading to new capabilities in quantum computation, quantum simulation, and precision sensing.

DOI: [10.1103/PhysRevA.91.063835](https://doi.org/10.1103/PhysRevA.91.063835)

PACS number(s): 42.50.Wk, 03.67.-a, 37.10.Jk, 85.85.+j

I. INTRODUCTION

Mechanical oscillators, such as microcantilevers, have demonstrated remarkable force sensitivity, enabling the detection of single-electron spins in solids [1] and tests for non-Newtonian gravity at submillimeter length scales [2]. Cantilevers that utilize strong magnetic gradients can achieve excellent spatial localization, allowing nanoscale magnetic resonance imaging [3,4]. A mechanical resonator coated with ferromagnetic material was recently used to coherently control the spin state of a single nitrogen-vacancy (NV) center in a diamond substrate [5], allowing sensitive scanning magnetometry with nanometer spatial resolution. NV centers have also been used to coherently sense the motion of a magnetized cantilever beam [6]. Scanning NV magnetometry has been used to detect single-electron spins under ambient conditions [7]. It has been proposed that mechanical resonators loaded with a magnetic tip could be interfaced with Bose-Einstein condensates (BECs) [8,9] or single atoms to implement quantum gates [10]. Coupling of cantilevers to atoms has been demonstrated using magnetic interactions for room-temperature atomic gases [11] and using surface forces for BECs [12], important steps toward the goal of probing and manipulation of atomic spins with micrometer-scale resolution and single-spin sensitivity. Here we demonstrate magnetic coupling of a cantilever to an ensemble of cold atoms. This approach provides a different set of advantages and challenges than other techniques involving coupling to spins in solid-state systems.

Such mechanical spin-exchange coupling can be coherent and nondestructive. Advances in this area could lead to new capabilities in neutral atom quantum computation and quantum simulation, microscopy and magnetic resonance force microscopy, precision force sensing, or atomic clocks that couple mechanics to an atomic resonance [13]. For instance, optical lattices can confine regular arrays of atoms where large subsets of atoms can be entangled, making these systems well suited for measurement-based quantum

computation schemes [14,15]. A scalable method to couple atoms occupying individual lattice sites with an array of cantilevers has been described [10]. Here each lattice site in a two-dimensional plane is paired with a magnetic cantilever tip to allow massively parallel single-qubit operations. The interaction of the cantilever with the atomic spin can be fully coherent, making this system promising for protocols requiring multiple manipulations on a single qubit.

Mechanical resonators can be used for quantum simulation protocols [16–18], in which arrays of individual neutral atoms are confined in large two-dimensional lattices. Using the mechanical approach, both the site population and spin state can, in principle, be determined, while complications involving light assisted collisions [19] that occur for optical readout methods can be avoided. It is possible to confine atoms using surface plasmonic modes in order to achieve submicron lattice spacing, allowing very fast tunneling rates [20]. Mechanical resonators could provide high-resolution imaging in such systems, without being limited by optical diffraction.

In this paper, we report on progress toward these goals by demonstrating the excitation of magnetic resonance in an ensemble of laser-cooled trapped Rb atoms using a microcantilever with a magnetic tip. The coupling is observed by measuring the loss from a magnetic trap as the oscillating cantilever induces Zeeman-state transitions in the atoms. The cantilever is mounted on a multilayer atom chip designed to capture, cool, and magnetically transport cold atoms. We also show that for realistic parameters, mechanical detection of individual atomic spins should be possible in a cryogenic system.

II. EXPERIMENTAL SETUP

In the experiment, Rb atoms emerge from a dispenser located approximately 5 cm from the chip surface and are collected in a mirror-magneto-optical trap (mirror-MOT) [21] approximately 2.5 mm above the chip surface. A portion of the chip surface is coated with 500 nm of Cu to provide a mirror for the MOT beams. Cu is chosen to minimize adsorption of Rb on the surface [22]. Following this initial MOT stage, which employs an external anti-Helmholtz field to generate a trap gradient of 10 G/cm, the MOT is transferred ~1.1 mm closer to the chip surface in a U-MOT stage,

*ageraci@unr.edu

[†]Present address: Department of Physics, Stanford University, Stanford, California 94305, USA.

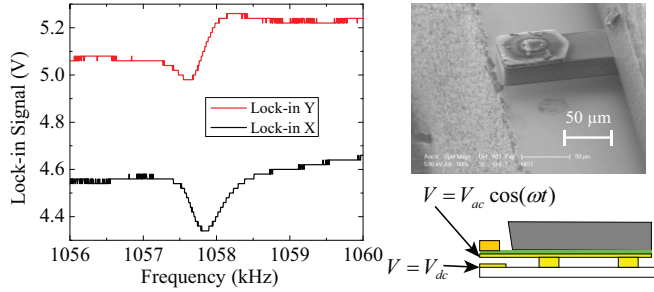


FIG. 1. (Color online) (left) Cantilever resonance as measured with a quadrant photodetector and lock-in amplifier. The red upper curve and black lower curve depict the Y and X quadratures of the lock-in signal, respectively. (top right) SEM micrograph of Si cantilever beam with CoNiMnP magnet. (bottom right) Schematic of capacitive driving mechanism.

where the gradient is provided by current in a U-shaped wire embedded in the chip and the atom number is approximately 5×10^6 . Following this stage, the atom cloud is compressed by reducing the hyperfine repump intensity, further cooled to $7 \mu\text{K}$ by polarization gradient cooling, and then optically pumped to the ^{87}Rb $|F = 2, m_F = 2\rangle$ hyperfine ground state for magnetic trapping. The atoms are then loaded into a magnetic quadrupole U trap produced by the same U-shaped wire used to create the U-MOT. Transferring the cold atoms from the U trap to the cantilevers is facilitated by magnetic guiding above the chip, which involves transport over a distance of approximately 0.8 cm on a time scale of 200 ms . The guiding field is produced by external magnetic fields and by current running through different wire configurations on the chip. During the transfer process it is necessary to change the axis of the trap to be parallel with the wire guides which lead to the cantilever. This rotation is accomplished with a P-shaped magnetic trap similar to that described in Ref. [23].

The Si cantilevers which are mounted on the atom-chip are shown in Fig. 1. They were fabricated at NIST by patterning and etching a silicon-on-insulator (SOI) wafer. They have dimensions of $130 \times 60 \times 25 \mu\text{m}$ and are functionalized with an electroplated CoNiMnP [24] ferromagnet of dimensions $85 \times 60 \times 9 \mu\text{m}$ with a total moment of approximately $2 \times 10^{-9} \text{ J/T}$, measured in a commercial magnetometer. The magnet is magnetized with its moment extending outward from the cantilever tip. The measured coercive field is sufficiently high that we expect the magnet to retain its moment throughout the experiment. The measured Q factor of the cantilevers ranges from 20 000 to 30 000 unloaded and is reduced to approximately 10^4 with the addition of the magnet. This Q factor is consistent with the theoretical limit calculated from thermoelastic dissipation [25]. The bare cantilevers are annealed in a nitrogen atmosphere at $700 \text{ }^\circ\text{C}$ for 1 h to improve the Q factor. Prior to annealing, the measured Q typically ranges from 3000 to 4000. The cantilevers are coated with gold following the annealing procedure, which typically reduces the Q factor to below 10^4 . For the cantilevers used in this work, the magnet is attached to the cantilever after the metallization step.

After magnetic transport, the atoms are trapped approximately $100 \mu\text{m}$ from the cantilever tip in a quadrupole trap formed by the magnetic tip itself and external fields. At this

point the atom temperature has increased to $\sim 100 \mu\text{K}$, and the trapped atom number is near 2×10^4 , as determined by absorption imaging. Once the atoms are trapped near the tip, those atoms in a “resonant slice” with a Larmor frequency that matches the cantilever vibrational frequency will have their spin undergo a coherent precession about the net direction of the total magnetic field, resulting in Zeeman-state transitions. The dc magnetic field from the cantilever moment combines with the external magnetic field to determine the Larmor precession frequency. The cantilever fundamental-mode resonance frequency when loaded with a magnet of mass M satisfies $\omega_c = \frac{k}{0.24m_c + M}$ for a cantilever of mass m_c . Here the spring constant $k = \frac{1}{4} E w (\frac{h}{l})^3$, where E is the Young’s modulus and l , w , and h are the cantilever length, width, and height, respectively. The measured resonance frequency of the loaded cantilever is 1057.7 kHz , in reasonable agreement with the expected value. The motion of the magnet is transduced into a transverse rf magnetic field, and the Rabi-frequency Ω_R for driven Zeeman spin transitions depends linearly on the amplitude of the cantilever motion δz as

$$\Omega_R = \delta z G_m \gamma, \quad (1)$$

where G_m is the gradient of the transverse component of the tip magnetic field along the direction of cantilever motion and γ is the gyromagnetic factor for ^{87}Rb , 7 Hz/nT . To efficiently observe the influence of the cantilever on the atomic spins, the Rabi frequency should be of the order of the average trap frequency, $\sim 1 \text{ kHz}$, as determined by numerical simulation for an atom with a temperature of $100 \mu\text{K}$ in the quadrupole trap. For our magnetic moment of $2 \times 10^{-9} \text{ J/T}$, the required cantilever amplitude is approximately 50 nm .

To characterize the motion of the cantilever *in situ*, a HeNe laser is reflected from the surface of the cantilever onto a quadrant photodetector with a bandwidth of 1 MHz . The quadrant photodetector is positioned on a two-dimensional stage with micrometers to allow a distance calibration. The motion is measured using an rf lock-in amplifier. The cantilever used in these measurements has a mechanical linewidth of $0.67 \pm 0.02 \text{ kHz}$ as determined by a Lorentzian fit to the data shown in Fig. 1. The cantilever is driven by applying ac + dc voltage between its metallized undersurface and a nearby electrode. For $V_{dc} = 40 \text{ V}$, $V_{ac} = 10 \text{ V}$, and electrode separation $d = 9 \mu\text{m}$, we measure a tip amplitude of approximately $\delta z = 34 \pm 13 \text{ nm}$ at 1057.7 kHz , sufficient to generate Rabi frequencies exceeding 100 Hz . The uncertainty in δz is dominated by the finite laser waist size at the cantilever tip, which is comparable to the cantilever width. Reduced uncertainty could be achieved by using a tighter focus or a fiber-coupled laser interferometer. Approximating the system as a parallel-plate capacitor, the expected amplitude is given by $\delta z = \frac{Q}{k} \frac{\epsilon_0 A V_{dc} V_{ac}}{d^2}$, where A is the effective area of the plates. Taking the measured Q factor, we calculate an expected tip displacement of $\delta z = 40 \text{ nm}$, which agrees with the measured result.

The effect of the cantilever motion on the atomic spins in the quadrupole trap can be more rigorously calculated using Landau-Zener theory [26,27]. For example, atoms beginning in the state $|F = 2, m_F = 2\rangle$ will experience a transition into the level $|F = 2, m_F = 1\rangle$ with a probability $P = 1 - \exp[-\frac{\pi \hbar \Omega_R^2}{\mu_B B' v}]$ as they traverse the resonant slice with

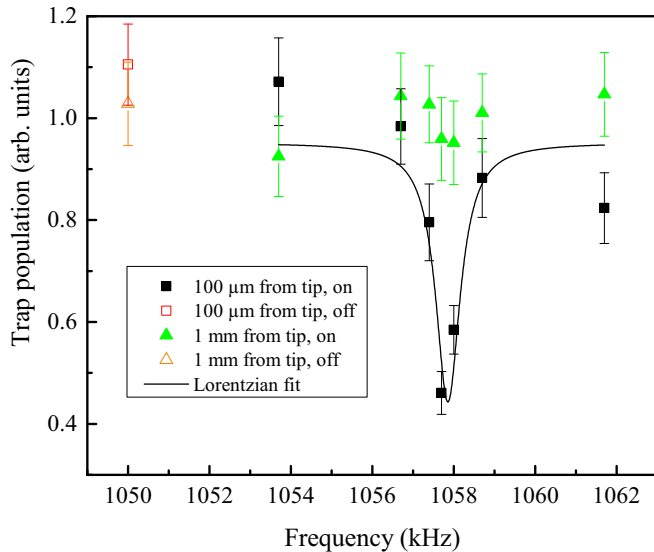


FIG. 2. (Color online) Atomic population in the trap determined by absorption imaging, after interacting with the cantilever for 11 ms at a distance of approximately $100 \mu\text{m}$ (black squares). When the cantilever is driven near its resonance of 1057.7 kHz, the trap population decreases (black squares). The open points indicate the population with the cantilever not capacitively driven. A Lorentzian fit to the peak is shown, which agrees with the measured linewidth of the cantilever resonance to within error bars. Also shown are data for the atoms separated from the cantilever by a larger distance of 1 mm (solid green triangles). As expected, no significant reduction in trap population occurs in this case.

velocity v . Here B' is the magnetic field gradient due to the cantilever tip, of the order of 10 T/m at the resonant slice nearest the cantilever. The gradient from the magnetic tip scales as $\sim r^{-4}$ for atom-tip separations r of the order of the size of the magnetic particle or larger. We model the magnetic field of the magnet assuming a rectangular geometry. One-dimensional numerical simulations indicate that for a thermal ensemble at $100 \mu\text{K}$, population loss due to the transition into strong-magnetic-field-seeking states can be expected over a time scale of ~ 10 ms for our experimental parameters [28].

III. RESULTS

The interaction with the cantilever becomes significant when the atomic cloud is moved to approximately $100 \mu\text{m}$ from the oscillating cantilever tip. After a variable time t of interaction, a low-intensity laser is used to probe the trap population via absorption imaging. A frame-transfer Peltier-cooled CCD camera is used for imaging in a differential imaging mode. A hyperfine depumping pulse is applied between the images which optically pumps atoms into the $F = 1$ state, which is a dark state for the imaging light. Figure 2 shows the trap population after $t = 11$ ms of interaction with the cantilever driven with $V_{\text{ac}} = 10$ V and $V_{\text{dc}} = 40$ V. We define time $t = 0$ as the approximate time that the atomic cloud centroid approaches $100 \mu\text{m}$ from the tip. The population remains relatively constant when the cantilever is not driven or driven off resonance. When the cantilever is driven on

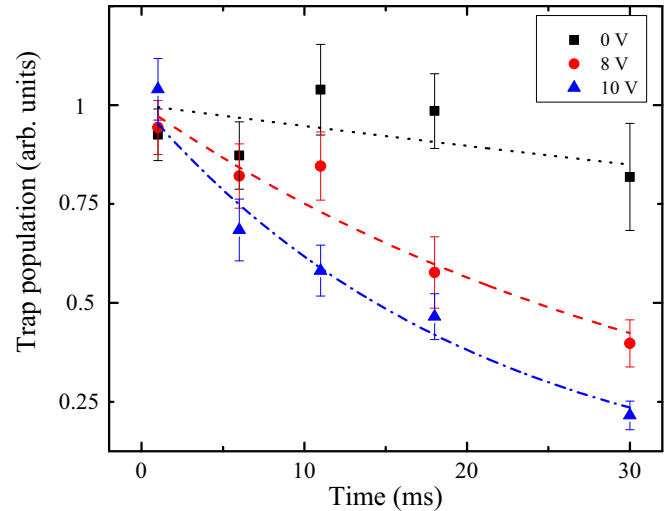


FIG. 3. (Color online) Relative trap population after the atomic cloud has interacted with the cantilever for varying times for two different amplitudes of cantilever motion (8 and 10 V) and with the cantilever not driven (0 V). Also shown are fitted exponential decay curves for each case.

resonance, the population gets reduced by approximately half. The population reduction is consistent with one-dimensional Landau-Zener simulations, to within the uncertainty of the measurements. A Lorentzian fit of the peak with fitted width 0.73 ± 0.3 kHz agrees with the measured linewidth of the cantilever resonance. With the cloud trapped at larger separation from the cantilever (approximately 1 mm) we observe no significant reduction in the trap population, as expected, due to the steep reduction in Rabi frequency at larger distances.

In Fig. 3 we show the trap population after interacting with the cantilever for a varying time at a distance of approximately $100 \mu\text{m}$. Results are shown for the cantilever driven with $V_{\text{ac}} = 0, 8,$ and 10 V (with V_{dc} constant at 40 V). The results again are suggestive of trap loss due to magnetic Zeeman transitions. We expect the transition probability to vary quadratically with the cantilever driving voltage over this range of interaction strength. Considering the calculated probability of undergoing a spin flip per pass of the atom through the resonant slice and the approximate expected rate of crossing due to the atomic motion, the data are in reasonable qualitative agreement with theoretical expectations from the one-dimensional (1D) Landau-Zener model. The fitted observed trap population decay times of 21 ± 3.1 and 34 ± 3.6 ms agree with the 1D model predictions to within a factor of approximately 2. As the actual atomic motion in the trap occurs in three dimensions and can be quite complex, we do not expect exact quantitative agreement for the 1D calculation. We also include an exponential decay fit to the case with $V_{\text{ac}} = 0$, which yields a significantly longer time constant, 184 ± 66 ms, in agreement with the measured magnetic trap lifetime.

IV. SPIN DETECTION

In this work we have demonstrated the ability to induce Zeeman-state transitions in trapped cold atoms using the oscillating cantilever tip. It is also interesting to consider

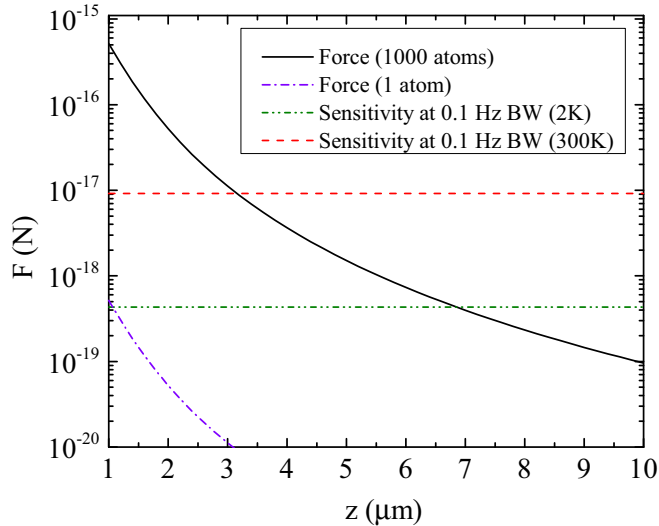


FIG. 4. (Color online) Thermal noise-limited force sensitivity in a 0.1-Hz bandwidth for a cantilever as described in the text and force due to the precession of 10^3 atomic spins (solid line) and a single spin (dash-dotted line) as a function of separation distance z from the center of the cantilever magnet.

detecting the precessing spins by observing the force they impart on the cantilever. A requirement for detecting the back-action of the atomic spins onto the cantilever is that the force induced must exceed the thermal noise-limited force sensitivity of the cantilever. The minimum detectable force due to the presence of thermal noise in a cantilever beam with natural frequency ω_c can be expressed as

$$F_{\min} = [4kk_B T b / \omega_c Q]^{1/2}, \quad (2)$$

where b is the bandwidth of the measurement, k is the spring constant, and T is the effective temperature of the mode under consideration. The cantilevers used in this work carry a large magnet to facilitate easier atomic trapping and have not been optimized for detecting the force from atomic spins on the cantilever. To investigate spin detection, we can utilize smaller, lower- k cantilevers to allow larger cantilever displacements. For example, with a SiN cantilever with dimensions $50 \times 1.1 \times 0.2 \mu\text{m}$ and loaded with a CoNiMnP electroplated magnet of dimensions $1.1 \times 0.9 \times 0.7 \mu\text{m}$, the resonance frequency is $\omega_c = 2\pi \times 70 \text{ kHz}$. Si cantilevers of similar size have been demonstrated with Q factors exceeding 380 000 [29]. Assuming $Q = 10^5$, the sensitivity at room temperature of such a cantilever is $\sim 29 \text{ aN/Hz}^{1/2}$, enabling the detection of 80 atomic (electron) spins at $1.3 \mu\text{m}$ separation

in a 1-Hz bandwidth. Such small separation from a surface could be realized with an optical trap [30]. For cryogenic cantilevers at 2 K, the Q factor can be expected to increase. Assuming $Q = 300\,000$ at 2 K, the force sensitivity becomes $1.3 \text{ aN/Hz}^{1/2}$, allowing single-electron spin detection in an ~ 0.1 -Hz bandwidth at $1.1\text{-}\mu\text{m}$ tip-atom separation, as shown in Fig. 4. While demonstrated spin coherence times have been long in surface traps [31], at these distances the Casimir-Polder potential needs to be considered, as well as magnetic field noise due to thermal currents in nearby conducting surfaces [32,33]. For atom-surface separations of greater than $0.5 \mu\text{m}$ these effects can be mitigated for suitable material thicknesses and conductivities [10].

V. DISCUSSION

We have demonstrated the manipulation of the hyperfine Zeeman states of magnetically trapped ^{87}Rb atoms using a driven cantilever beam functionalized with a magnetic tip. With optically trapped atoms and improved imaging, coherent control of single trapped atomic spins should be possible in a similar setup. Using a suitably scaled cryogenic setup, the spin of cold atoms can be sensed by measuring the force they exert on a microcantilever, with the possibility of single-spin sensitivity for realistic experimental parameters. Such cantilevers could be useful for quantum simulators in which arrays of individual neutral atoms are confined in large two-dimensional lattices. It has been shown theoretically that magnetic cantilevers can couple to ultracold atoms at micron distances in a regime analogous to the strong-coupling regime of cavity QED [8]. If the mechanical oscillators can be cooled to their quantum ground state [34–36], nonclassical states of the atomic degrees of freedom can be transferred to the motional states of the resonators and vice versa, with applications in quantum information science [10,37,38]. In these setups, mechanical oscillators can provide coupling between photons, spins, and charges via phonons [39–42]. Such transducers could be useful for quantum networks by allowing coupling between different types of quantum systems, each with different advantages.

ACKNOWLEDGMENTS

The authors thank Y.-J. Wang for experimental assistance during the early stages of this work. We thank P. Treutlein, and J. Weinstein for useful discussions. This work was supported in its early stages by DARPA. A.G. is supported in part by Grant No. NSF-PHY 1205994. This work is a partial contribution of NIST and is therefore not subject to copyright in the United States.

-
- [1] D. Rugar, R. Budakian, H. J. Mamin, and B. W. Chui, *Nature (London)* **430**, 329 (2004).
 - [2] A. A. Geraci, S. J. Smullin, D. M. Weld, J. Chiaverini, and A. Kapitulnik, *Phys. Rev. D* **78**, 022002 (2008).
 - [3] C. L. Degen, M. Poggio, H. J. Mamin, C. T. Rettner, and D. Rugar, *Proc. Natl. Acad. Sci. USA* **106**, 1313 (2009).
 - [4] H. J. Mamin, M. Kim, M. H. Sherwood, C. T. Rettner, K. Ohno, D. D. Awschalom, and D. Rugar, *Science* **339**, 557 (2013).
 - [5] S. Hong, M. S. Grinolds, P. Maletinsky, R. L. Walsworth, M. D. Lukin, and A. Yacoby, *Nano Lett.* **12**, 3920 (2012).
 - [6] S. Kolkowitz, A. C. Bleszynski Jayich, Q. P. Unterreithmeier, S. D. Bennett, P. Rabl, J. G. E. Harris, and M. D. Lukin, *Science* **335**, 1603 (2012).
 - [7] M. S. Grinolds, S. Hong, P. Maletinsky, L. Luan, M. D. Lukin, R. L. Walsworth, and A. Yacoby, *Nat. Phys.* **9**, 215 (2013).

- [8] P. Treutlein, D. Hunger, S. Camerer, T. W. Hansch, and J. Reichel, *Phys. Rev. Lett.* **99**, 140403 (2007).
- [9] Z. Darázs, Z. Kurucz, O. Kalman, T. Kiss, J. Fortagh, and P. Domokos, *Phys. Rev. Lett.* **112**, 133603 (2014).
- [10] A. A. Geraci and J. Kitching, *Phys. Rev. A* **80**, 032317 (2009).
- [11] Y.-J. Wang, M. Eardley, S. Knappe, J. Moreland, L. Hollberg, and J. Kitching, *Phys. Rev. Lett.* **97**, 227602 (2006).
- [12] D. Hunger, S. Camerer, T. W. Hansch, D. König, J. P. Kotthaus, J. Reichel, and P. Treutlein, *Phys. Rev. Lett.* **104**, 143002 (2010).
- [13] C. D. White, G. Piazza, P. J. Stephanou, and A. P. Pisano, *Sens. Actuators A* **134**, 239 (2007).
- [14] G. K. Brennen, C. M. Caves, P. S. Jessen, and I. H. Deutsch, *Phys. Rev. Lett.* **82**, 1060 (1999).
- [15] O. Mandel, M. Greiner, A. Widera, T. Rom, T. W. Hansch, and I. Bloch, *Nature (London)* **425**, 937 (2003).
- [16] M. Lewenstein, A. Sanpera, V. Ahufinger, B. Damski, A. Sen(De), and U. Sen, *Adv. Phys.* **56**, 243 (2007).
- [17] I. Bloch, J. Dalibard, and W. Zwerger, *Rev. Mod. Phys.* **80**, 885 (2008).
- [18] W. S. Bakr, J. I. Gillen, A. Peng, S. Fölling, and M. Greiner, *Nature (London)* **462**, 74 (2009).
- [19] W. S. Bakr, P. M. Preiss, M. Eric Tai, R. Ma, J. Simon, and M. Greiner, *Nature (London)* **480**, 500 (2011).
- [20] M. Gullans, T. G. Tiecke, D. E. Chang, J. Feist, J. D. Thompson, J. I. Cirac, P. Zoller, and M. D. Lukin, *Phys. Rev. Lett.* **109**, 235309 (2012).
- [21] J. Reichel, W. Hansel, and T. W. Hansch, *Phys. Rev. Lett.* **83**, 3398 (1999).
- [22] G. Biedermann (private communication).
- [23] R. Long, T. Rom, W. Hansel, T. W. Hansch, and J. Reichel, *Eur. Phys. J. D* **35**, 125 (2005).
- [24] H. J. Cho and C. H. Ahn, *J. Microelectromech. Syst.* **11**, 78 (2002).
- [25] K. Y. Yasumura, T. D. Stowe, E. M. Chow, T. Pfafman, T. W. Kenny, B. C. Stipe, and D. Rugar, *J. Microelectromech. Syst.* **9**, 32 (2000).
- [26] C. Zener, *Proc. R. Soc. London, Ser. A* **137**, 696 (1932).
- [27] J. R. Rubbmark, M. M. Kash, M. G. Littman, and D. Kleppner, *Phys. Rev. A* **23**, 3107 (1981); W. Ketterle and N. J. van Druten, *Adv. At. Mol. Opt. Phys.* **37**, 181 (1996).
- [28] M. D. Eardley (unpublished).
- [29] C. Degen (private communication).
- [30] J. D. Thompson, T. G. Tiecke, N. P. de Leon, J. Feist, A. V. Akimov, M. Gullans, A. S. Zibrov, V. Vuletic, and M. D. Lukin, *Science* **340**, 1202 (2013).
- [31] P. Treutlein, P. Hommelhoff, T. Steinmetz, T. W. Hansch, and J. Reichel, *Phys. Rev. Lett.* **92**, 203005 (2004).
- [32] Y. J. Lin, I. Teper, C. Chin, and V. Vuletic, *Phys. Rev. Lett.* **92**, 050404 (2004).
- [33] D. M. Harber, J. M. Obrecht, J. M. McGuirk, and E. A. Cornell, *Phys. Rev. A* **72**, 033610 (2005).
- [34] A. D. O'Connell, M. Hofheinz, M. Ansmann, R. C. Bialczak, M. Lenander, E. Lucero, M. Neeley, D. Sank, H. Wang, M. Weides, J. Wenner, J. M. Martinis, and A. N. Cleland, *Nature (London)* **464**, 697 (2010).
- [35] J. D. Teufel, T. Donner, D. Li, J. W. Harlow, M. S. Allman, K. Cicak, A. J. Sirois, J. D. Whittaker, K. W. Lehnert, and R. W. Simmonds, *Nature (London)* **475**, 359 (2011).
- [36] J. Chan, T. P. Mayer Alegre, A. H. Safavi-Naeini, J. T. Hill, A. Krause, S. Gröblacher, M. Aspelmeyer, and O. Painter, *Nature (London)* **478**, 89 (2011).
- [37] A. Jöckel, A. Faber, T. Kampschulte, M. Korppi, M. T. Rakher, and P. Treutlein, *Nat. Nanotechnol.* **10**, 55 (2015).
- [38] C. K. Law and J. H. Eberly, *Phys. Rev. Lett.* **76**, 1055 (1996).
- [39] K. Stannigel, P. Rabl, A. S. Sorensen, P. Zoller, and M. D. Lukin, *Phys. Rev. Lett.* **105**, 220501 (2010).
- [40] C. A. Regal and K. W. Lehnert, *J. Phys. Conf. Ser.* **264**, 012025 (2011).
- [41] A. H. Safavi-Naeini and O. Painter, *New J. Phys.* **13**, 013017 (2011); P. Rabl, S. J. Kolkowitz, F. H. L. Koppens, J. G. E. Harris, P. Zoller, and M. D. Lukin, *Nat. Phys.* **6**, 602 (2010).
- [42] E. Verhagen, S. Deleglise, S. Weis, A. Schliesser, and T. J. Kippenberg, *Nature (London)* **482**, 63 (2012).